OAK RIDGE NATIONAL LABORATORY LIBRARIES
3 4456 0551428 0

ORNL/TM-6370

Comparative Studies of Head-End Processing Using Irradiated, Mechanically Blended and Coprecipitated $(U,Pu)O_2$ Reactor Fuels

J. H. Goode
R. G. Stacy

[redacted]

OAK RIDGE NATIONAL LABORATORY
CENTRAL RESEARCH LIBRARY
CIRCULATION SECTION
4500N ROOM 175
LIBRARY LOAN COPY
DO NOT TRANSFER TO ANOTHER PERSON
If you wish someone else to see this report, send in name with report and the library will arrange a loan.
UCN 7969 (3 9-77)

OAK RIDGE NATIONAL LABORATORY
OPERATED BY UNION CARBIDE CORPORATION · FOR THE DEPARTMENT OF ENERGY

C.79c

Printed in the United States of America. Available from
the Department of Energy,
Technical Information Center
P.O. Box 62, Oak Ridge, Tennessee 37830
Price: Printed Copy $4.50; Microfiche $3.00

This report was prepared as an account of work sponsored by an agency of the United States Government. Neither the United States Government nor any agency thereof, nor any of their employees, contractors, subcontractors, or their employees, makes any warranty, express or implied, nor assumes any legal liability or responsibility for any third party's use or the results of such use of any information, apparatus, product or process disclosed in this report, nor represents that its use by such third party would not infringe privately owned rights.

ORNL/TM-6370
Dist. Category 79c

Contract No. W-7405-eng-26

ADVANCED FUEL RECYCLE PROGRAM

COMPARATIVE STUDIES OF HEAD-END PROCESSING USING IRRADIATED, MECHANICALLY BLENDED AND COPRECIPITATED $(U,Pu)O_2$ REACTOR FUELS

J. H. Goode
R. G. Stacy

Chemical Technology Division

Date Published - September 1978

NOTICE This document contains information of a preliminary nature. It is subject to revision or correction and therefore does not represent a final report.

OAK RIDGE NATIONAL LABORATORY
Oak Ridge, Tennessee 37830
operated by
UNION CARBIDE CORPORATION
for the
DEPARTMENT OF ENERGY

OAK RIDGE NATIONAL LABORATORY LIBRARIES

3 4456 0551428 0

CONTENTS

PAGE

ABSTRACT 1

1. INTRODUCTION 1

2. EXPERIMENTAL 2

3. RESULTS. 4

3.1 Shearing 4
3.2 Voloxidation 4
3.2.1 Material balances and weight gains during oxidation 7
3.2.2 Comminution of fuel during voloxidation 7
3.2.3 Gaseous release profiles 9
3.2.4 Rate of oxygen consumption 12
3.2.5 Release of gaseous fission products 13
3.2.6 Fission product distribution during voloxidation 14
3.2.7 Discussion of voloxidation results 19
3.3 Dissolution Studies 23
3.3.1 Leaching procedure 23
3.3.2 Material balances 24
3.3.3 Solubility of uranium and plutonium 24
3.3.4 Ionic analyses of NUMEC dissolver solutions . . 24
3.3.5 Dissolution residues 28
3.3.6 Isotopic composition of NUMEC fuel rods 28
3.3.7 Stability of dissolver solutions 31
3.3.8 Fission product content of NUMEC rods 31
3.3.9 Tritium distribution 35
3.3.10 Distribution of fission products during dissolution. 36

4. CONCLUSIONS. 36

5. ACKNOWLEDGMENTS 38

6. REFERENCES 39

COMPARATIVE STUDIES OF HEAD-END PROCESSING USING IRRADIATED, MECHANICALLY BLENDED AND COPRECIPITATED $(U,Pu)O_2$ REACTOR FUELS

J. H. Goode
R. G. Stacy

ABSTRACT

A series of experiments was performed with highly irradiated $(U,Pu)O_2$ to determine the effects of voloxidation on the release of fission products and on the subsequent dissolution characteristics. It was found that voloxidation was more effective at 600 than at 650°C for releasing the gaseous fission products ^{3}H, ^{14}C, and ^{85}Kr from the experimental fuels. The lower-temperature treatment released about 95% of the tritium, 97 to 98% of the ^{14}C, and about 56% of the ^{85}Kr. Less than 1% of the ^{106}Ru, ^{125}Sb, or ^{144}Ce were released, but up to 6% of the $^{134-137}Cs$ was volatilized; most of the cesium deposited on the walls of the voloxidizer. Up to 80% of the ^{129}I was released, and most of it was carried into the off-gas system where it was sorbed onto activated charcoal. The voloxidizer at both temperatures generated a larger weight (1.5 to 2.2 times) of nitric acid insoluble residue than unvoloxidized $(U,Pu)O_2$. After voloxidation, the nitric acid insoluble residue also contained more plutonium than did the residue produced in the absence of voloxidation; another leach with 8 M HNO_3--0.05 M KF dissolved the plutonium.

1. INTRODUCTION

This document describes additional hot-cell tests with highly irradiated $(U,Pu)O_2$ to determine the effects of high-temperature oxidation (voloxidation) on the volatilization of fission products and on the dissolution of the oxidized fuel in nitric acid. The Nuclear Materials and Equipment Corporation (NUMEC) fabricated three replicate fuel assemblies containing 0.25-in.-OD stainless-steel-clad rods filled with 20% PuO_2--80% $^{235}UO_2$ pellets. They were to be irradiated in the Experimental Breeder Reactor No. 2 (EBR-2) to nominal burnup levels of 30,000, 60,000, and 100,000 MWd/ton.[1] The rods from Assembly A were removed at 33,000 MWd/ton, but the irradiation of Assemblies B and C was continued to well above 100,000 MWd/ton. An earlier report described experiments with the mechanically blended pellet portions of two of the fuel rods from the two high-burnup assemblies; one rod (B-7) was irradiated to a nominal 16.5-at. % burnup, and the other rod (C-13) was irradiated to a nominal 17.5-at. % burnup.[2] This report summarizes the

work with coprecipitated $(U,Pu)O_2$ from the same rods and compares the two types of fuels.

Each rod in each assembly contained a 14.5-in.-tall stack of about 28 pellets of each type (mechanically blended and coprecipitated mixed oxides) with a stack of axial-blanket UO_2 pellets on top of the mixed oxide pellets. Mechanical blending involves the milling or grinding together of UO_2 powder (in this case, enriched to 93% ^{235}U) with PuO_2 powder, pressing the mixture into pellets, and sintering the pellets. Coprecipitation involves blending together solutions of plutonium nitrate and uranyl nitrate, precipitating ammonium diuranate and plutonium hydroxide with ammonia gas, and filtering, washing, and drying the powder; the powder is then reduced with 8% hydrogen in nitrogen to $(U,Pu)O_2$, milled to form fine particles, and finally pressed into pellets.[1] Rods B-7 and C-13 were identical, and each contained coprecipitated and mechanically blended pellets from the same fabrication batches (Nos. 4 and 15 respectively). They differed only in burnup level. Fabrication details for the rods were described earlier.[1,2] The fuel in the rods is not representative of present-day manufacturing techniques, but rather is from an early stage of development.

The head-end (i.e., presolvent extraction) processing steps in the hot-cell tests included gamma spectrometry (scanning), puncturing to determine fission gas release, shearing the stainless-steel-clad rods, voloxidation of portions of the fuel segments, and dissolving the voloxidized and unvoloxidized portions to determine differences in behavior due to the fabrication, irradiation, and head-end treatment. The experimental equipment and methods were the same as reported for the mechanically blended fuel.[2] The integral gamma scans (>0.5 MeV) of the rods (Fig. 1) show that the $^{134-137}Cs$ in the rods migrated to the cooler zones during irradiation. The scan information is superimposed on a sketch of the loaded fuel rods.

2. EXPERIMENTAL

The fuel rods were cut in a single-pin hydraulic shear operated by a hand pump. Fuel dislodged from the cladding during shearing was characterized as to size distribution. The voloxidation was conducted in a batch-operated, rotating stainless steel voloxidizer (3.25 in. ID)

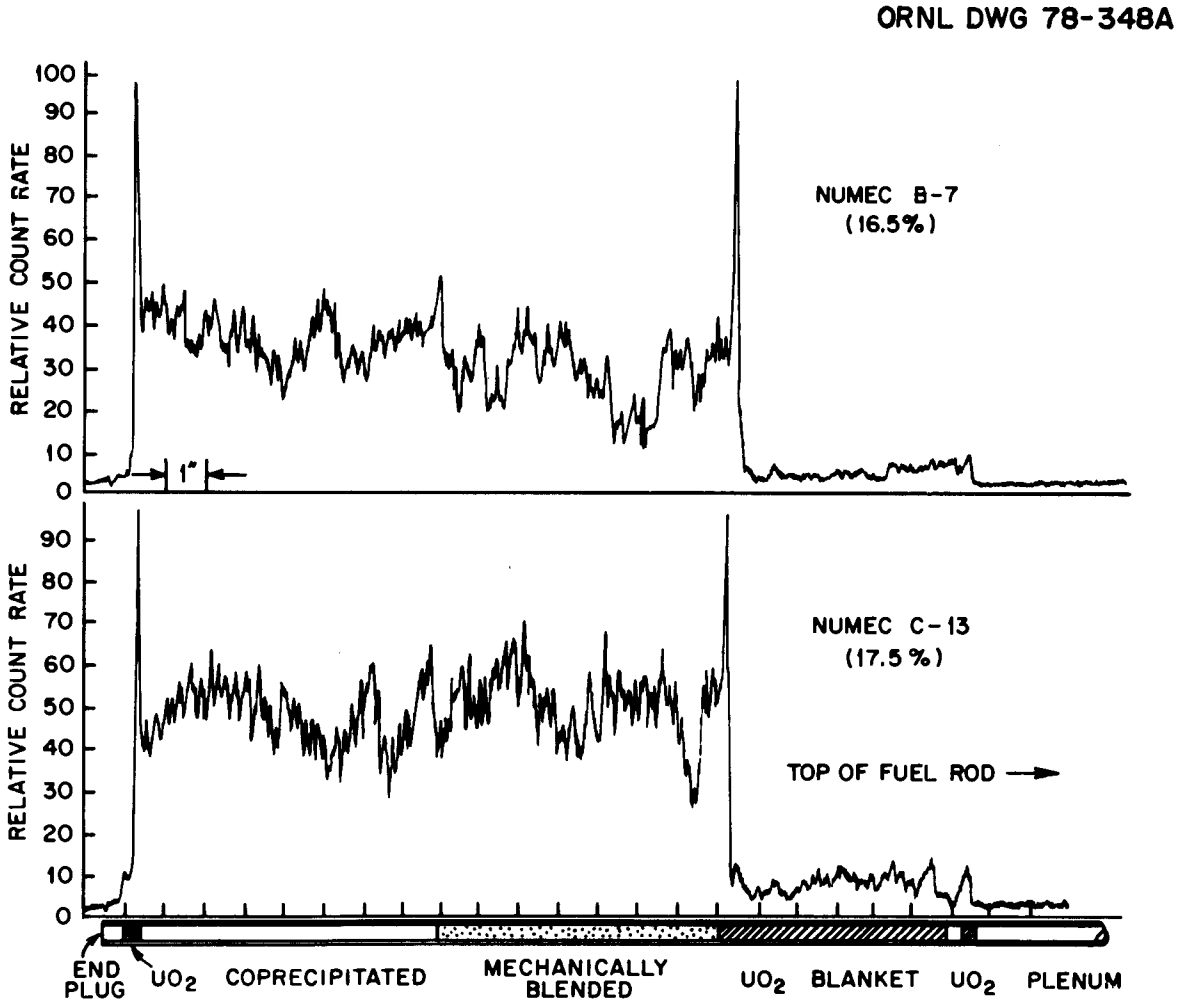

Fig. 1. Integral gamma scans of NUMEC fuel rods (>0.5 MeV).

equipped with a sintered stainless steel filter (35-μm porosity) at the gas inlet and outlet. The off-gases were cooled in the hollow shaft of the voloxidizer to about 125°C, which caused semivolatile fission products to deposit on tubing inserted into the shaft. The off-gases were sequentially passed through filters, charcoal beds to trap ^{129}I, hot copper oxide to oxidize tritium, molecular sieve and silica gel to remove tritiated water, a multichannel gamma spectrometer (MCA) for ^{85}Kr analysis, and collected for analysis of the total ^{14}C and ^{85}Kr content (Fig. 2).

The voloxidized fuel was sieved to determine the amount of comminution due to voloxidation and then leached three times with nitric acid to determine its solubility. The dissolution off-gases were scrubbed with sodium hydroxide to remove $^{3}H_2O$, $^{14}CO_2$, and ^{129}I, and were finally collected for ^{85}Kr determination. Material balances on the uranium, plutonium, and fission products were made by analyzing all of the solutions and solids generated in each experiment.

3. RESULTS

3.1 Shearing

The single-pin hydraulic shear was used to cut each 0.25-in. diam stainless-steel-clad rod into 0.5-in.-long segments for voloxidation and dissolution studies. A compilation of shearing data showing the amount of fuel released from each rod section is given in Table 1. Releases from the mechanically blended portions of mixed oxide (Fig. 1) were 10 to 12% of the total fuel contained in those sections for both rods, and averaged close to 0.35 g per cut (about 1% of the fuel) with each blade pass. The release of coprecipitated mixed oxide was 8% from rod B-7 and 21% from rod C-13; release from the blanket UO_2 was 12% from rod B-7 and 21% for rod C-13. In all cases, the amount of fuel released per cut was highest for the higher burnup rod (C-13). No significant difference appeared to be caused by the fabrication route of the pellets.

3.2 Voloxidation

As indicated in the earlier report,[2] the placing of two different fuel types within the 14.5-in. active length of the NUMEC fuel rods tended to obscure small effects near the boundaries between the

ORNL DWG. 77-616R3

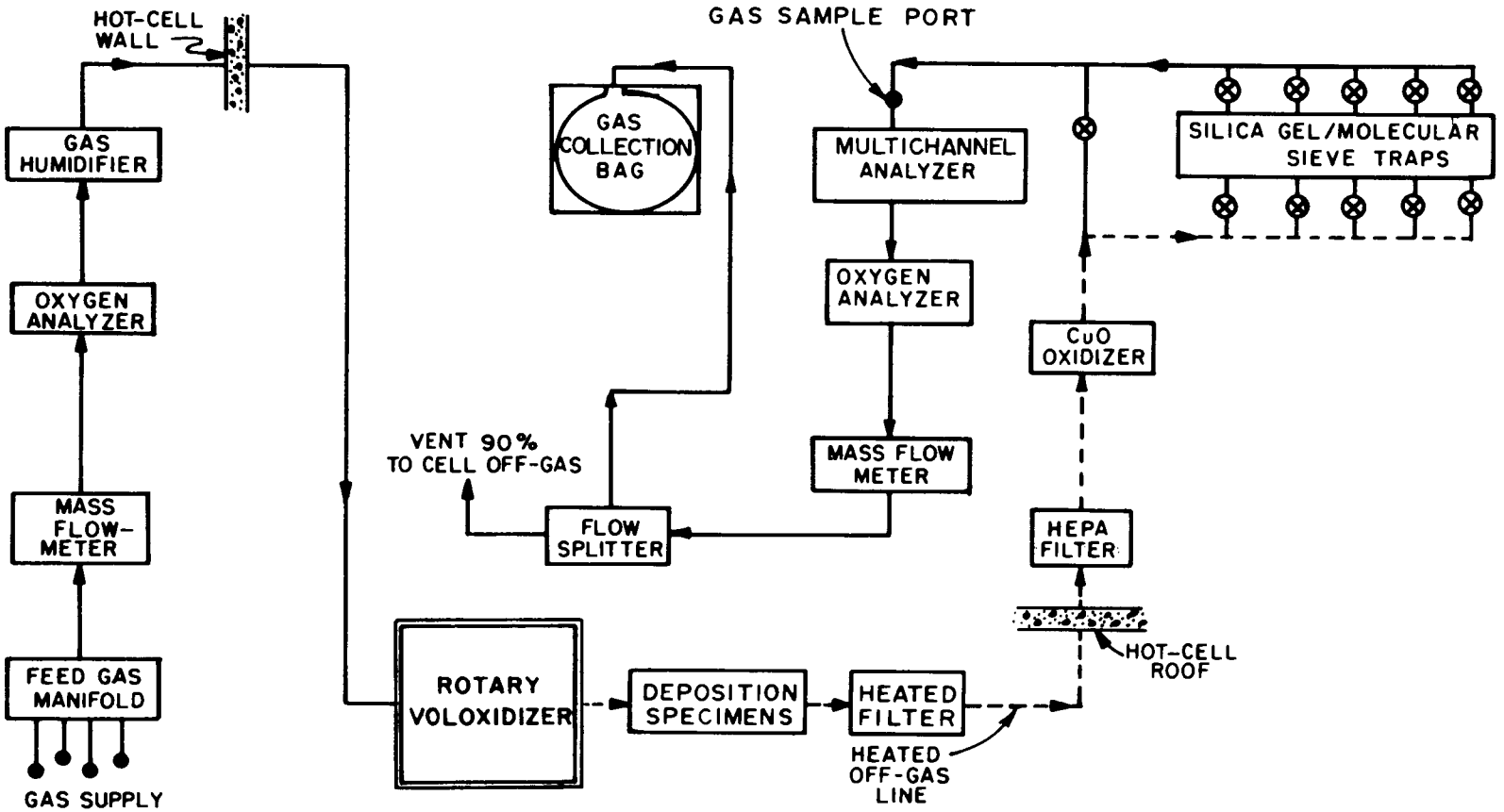

Fig. 2. Schematic diagram of voloxidation equipment.

coprecipitated, mechanically blended pellets, and the UO_2 blanket pellets. This resulted primarily because of mixing by diffusion during irradiation and the difficulty of locating the exact interface between the pellets during shearing. We will therefore present data from the experiments with both of the mixed-oxide-fuel types from the same rod; the data on the UO_2 blanket segments will be presented in a future report.

Table 1. Shearing irradiated NUMEC fuel rods

	Coprecipitated		Mechanically blended		Axial blanket	
	B-7	C-13	B-7	C-13	B-7	C-13
Avg force per cut, kg	215	212	167	167	379	292
Fuel wt, g	38.9	38.7	35.8	36.9	34.4	35.5
Dislodged by shearing, g	3.11	8.02	3.60	4.40	4.28	7.23
Dislodged, % total	8.0	20.7	10.1	11.9	12.4	20.4
Dislodged per cut, g	0.21	0.57	0.30	0.40	0.39	0.66
Dislodged per cut, %	0.51	1.50	0.83	1.08	1.10	1.86

The loading and operation of the voloxidizer for the experiments with stainless-steel-clad, coprecipitated $(U,Pu)O_2$ were the same as in previous runs with mechanically blended fuel[2] except that the voloxidation temperature was 600°C instead of 650°C. In all of the runs, the size distribution of the voloxidized product was measured prior to dissolution. Deposition samples were obtained from the voloxidizer and off-gas system to measure the extent of fission product "plateout." With the exception of run FBR-3, where the increase in the system back-pressure (after 20 min of operation) terminated the off-gas collection, the off-gases were monitored for gaseous radionuclide concentrations and continuously analyzed for oxygen content. Each run was continued beyond the point at which oxygen consumption had ended and the ^{85}Kr content in the off-gas had returned to near background levels.

For easy reference in the following sections, the run identifications and conditions for the voloxidation of the mechanically blended (MB) and coprecipitated (CP) fuels are given in Table 2.

Table 2. Identification of runs and voloxidation conditions

Run No.	Rod No.	Fuel type[a]	Charged to voloxidizer: Fuel wt[b] (g)	Charged to voloxidizer: No. of clad pieces[c]	Voloxidation conditions: Time (hr)	Voloxidation conditions: Temp (°C)	Voloxidation conditions: Atm[d]	Voloxidation conditions: Rotation (rpm)
FBR-1	B-7	MB	31.75	11	3.2	650	Air	12
FBR-2	C-13	MB	31.46	10	4.1	650	Air	12
FBR-3	B-7	CP	34.50	14	3.4	600	Air	12
FBR-4	C-13	CP	35.30	13	3.8	600	Air	12

[a]Mechanically blended fuel, MB; coprecipitated fuel, CP.
[b]Weight of oxide plus weight of fission products only.
[c]Each piece ∿0.5 in. long.
[d]Flow at 200 to 300 cm^3/min.

3.2.1 Material balances and weight gains during oxidation

The high burnup of fissile isotopes (∿17%) attained by the NUMEC rods made it necessary to account for the weight of fission products when calculating the amounts of heavy metal oxide in each voloxidizer charge and product. Calculations for the irradiation of 1 metric ton of this fuel using the ORIGEN computer code[3] showed:

Reactor input: 1136.4 kg $(U,Pu)O_2$ [1000 kg U + Pu]

Reactor output: 15.4 kg Xe + Kr (95% released during irradiation)

113.2 kg fission product oxides

1007.8 kg $(U,Pu)O_2$ [886.8 kg U + Pu]

1136.4 kg

Calculations[2] based on these amounts indicated that the weight of $(U,Pu)O_2$ was 89.84% of the total fuel weight entering the voloxidizer. A theoretical weight gain for conversion of the UO_2 in the $(U_{0.865},Pu_{0.135})O_2$ (postirradiation analysis) to U_3O_8 was calculated to be about 3.22%. Material balances for voloxidations of both fuel rods are shown in Table 3.

3.2.2 Comminution of fuel during voloxidation

Size distributions for the loose fuel charged into and recovered from the voloxidizer during the experiments at 600°C are listed in Table 4. It was previously shown that the voloxidation of the mechanically

Table 3. Material balances on voloxidation of NUMEC $(U,Pu)O_2$

	Run FBR-1 Rod B-7	Run FBR-2 Rod C-13	Run FBR-3 Rod B-7	Run FBR-4 Rod C-13
Input wt, g				
Total	40.40	40.20	44.10	43.40
Cladding	8.65	8.74	9.60	8.10
Fuel[a]	31.75	31.46	34.50	35.30
$(U,Pu)O_2$[b]	28.56	28.30	31.03	31.75
Output wt, g				
Total	40.90	40.70	44.90	43.40[c]
Cladding	8.65	8.74	9.60	8.10
Fuel[a]	32.25	31.96	35.30	35.30
Theoretical wt gain[d]	0.92	0.91	1.00	1.02
Actual wt gain, g	0.5	0.5	0.8	c
Conversion, % (calcd)[e]	~100.0	92.0	f	~110.0

[a]Includes weight of $(U,Pu)O_2$ plus weight of fission products.

[b]Weight of $(U,Pu)O_2$ = 0.8984 times the total fuel weight.

[c]Some product unrecovered due to handling losses.

[d]Based on 3.22% wt gain of $(U,Pu)O_2$ for full conversion of UO_2 to U_3O_8.

[e]Calculated from moles of O_2 consumed.

[f]Off-gas monitoring was interrupted during the run.

Table 4. Release of NUMEC coprecipitated $(U,Pu)O_2$ from 0.5-in.-long sheared, stainless steel cladding by voloxidation in air at 600°C

	Run No. FBR-3, Rod No. B-7		Run No. FBR-4, Rod No. C-13	
	In	Out	In	Out
Loose fuel,[a] g	3.11	26.4	8.02	29.2
Total, %	9.01	82.6	23.24	82.7
Mesh, %				
+35	59.8	55.6	69.7	61.5
+100	22.2	10.6	17.8	9.4
-100	18.0		12.5	
+325		14.8		12.1
-325		19.0		17.0

[a]Includes weight of fission products.

blended mixed oxide in air at 650°C increased the amount of loose fuel from ∿12 to 13% to ∿60 to 65% of the total.[2] The release of the coprecipitated fuel from the cladding by voloxidation in air at 600°C appeared to be even more complete; approximately 83% of the fuel was dislodged by the treatment. As before, most of the dislodged material was still in fairly large pieces (+35 mesh) indicating that the $(U,Pu)O_2$ material did not pulverize in either case.

3.2.3 Gaseous release profiles

Curves for the concentrations of tritium and krypton in the off-gas during the FBR-4 experiment are plotted as a function of run time in Fig. 3, and are related to the corresponding oxygen content of the voloxidizer off-gas. The cumulative oxygen consumption and fission gas release profiles (as percentages of amounts initially in the fuel) are shown in Fig. 4. Release curves for voloxidations of the mechanically blended $(U,Pu)O_2$ at 650°C were presented previously.[2]

The rate of release from the fuel at 600°C closely followed the rate at which oxygen was consumed. After 1.5 hr at temperature, most of the tritium in the fuel had been removed. At that point, the amount released was within 2% of the total removal level of 98% for the 600°C

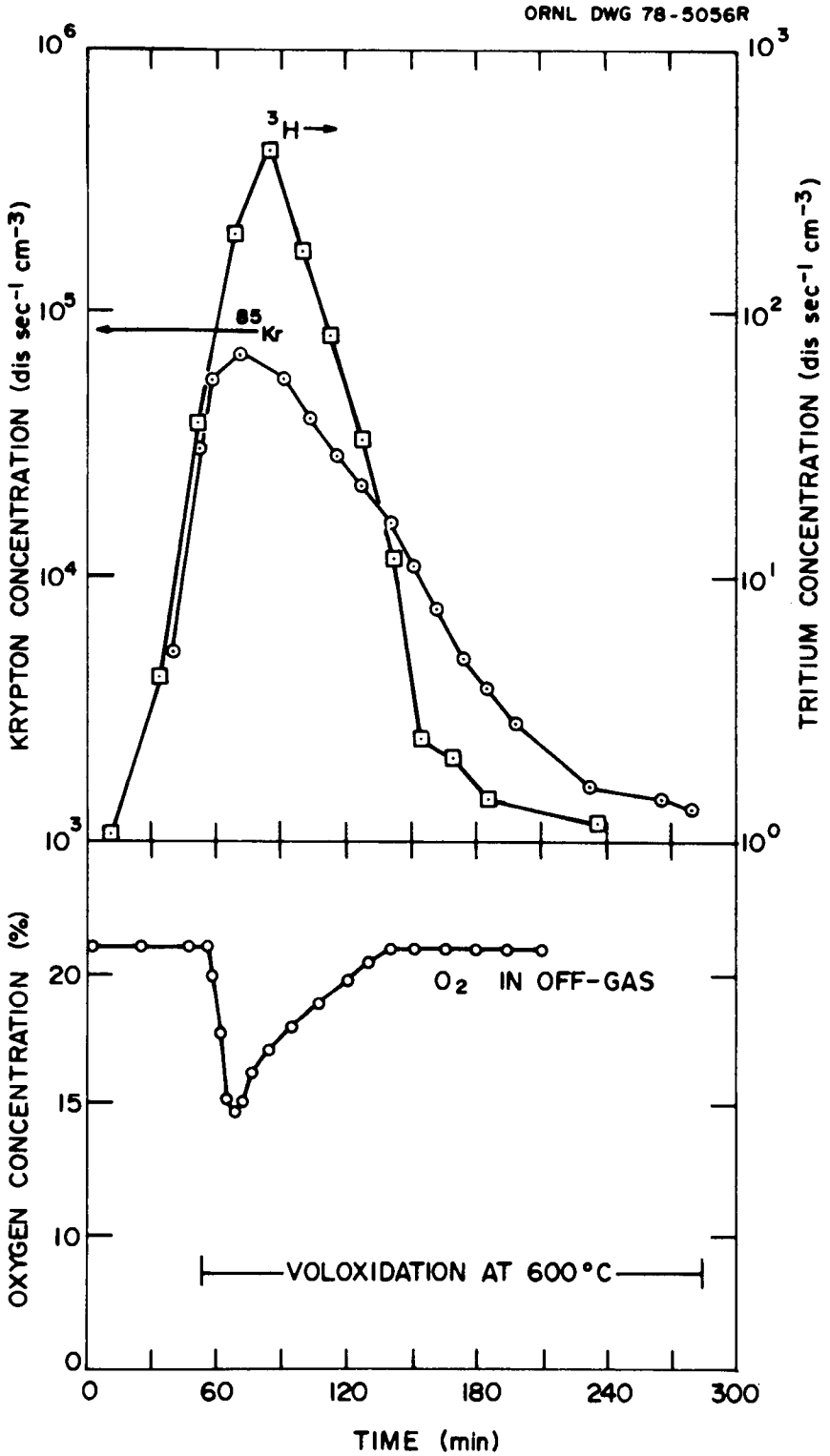

Fig. 3. Voloxidizer off-gas concentration profiles for tritium, krypton, and oxygen (FBR-4: air, 600°C).

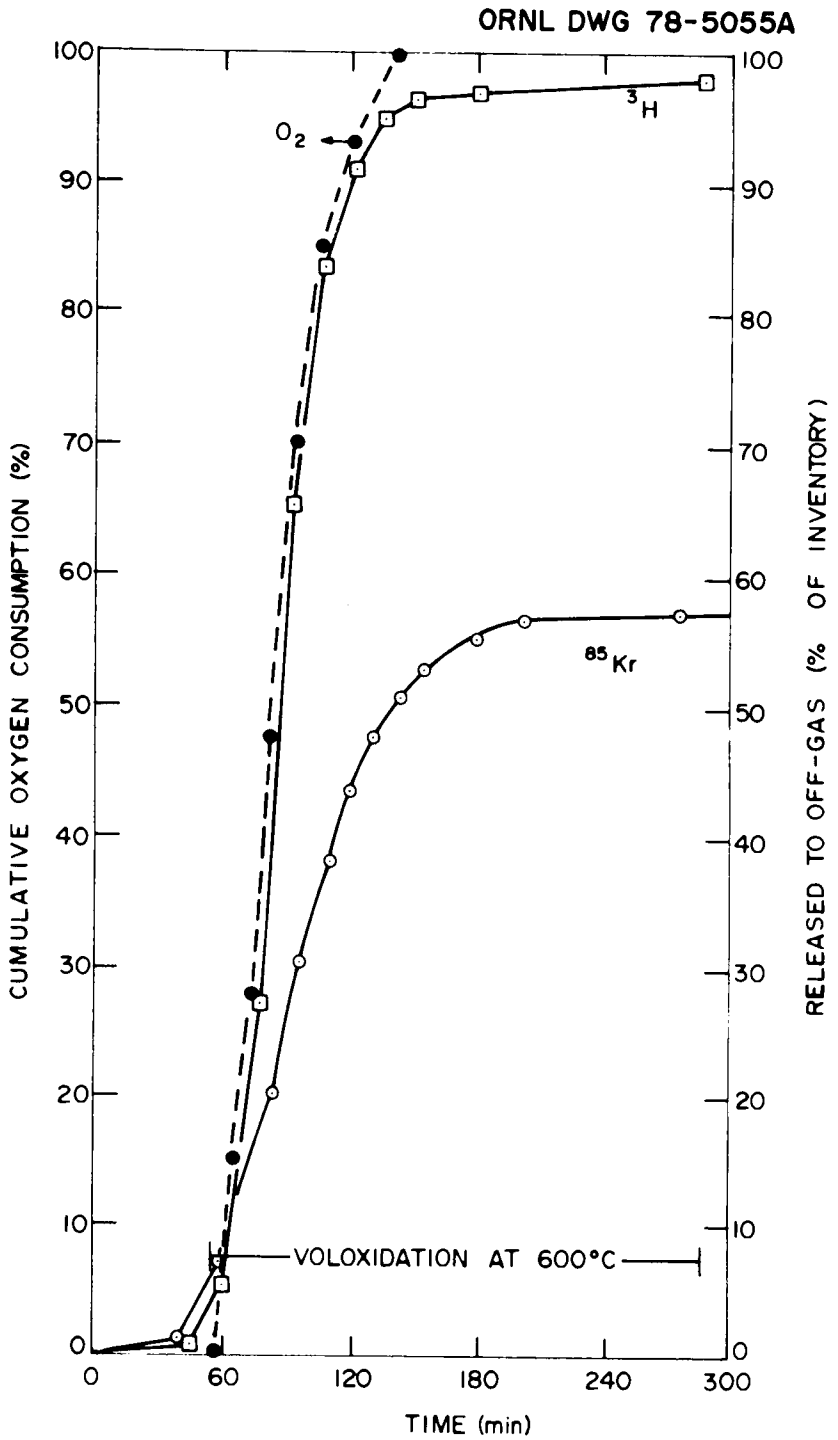

Fig. 4. Gaseous release and oxygen consumption during voloxidation (FBR-4: air, 600°C).

voloxidation. For the voloxidations at 650°C, tritium releases after 1.5 hr were about 10% less than the amount totally evolved, indicating slower releases at the higher temperature. Tritium recovered on traps during air purges of the system following each of the 600°C temperature runs amounted to about 0.2% of the total contained by the fuel. Approximately 2 to 3% of the inventory was collected via purging after the 650°C run. In each case, water and nitric acid rinses of the heated off-gas line following the run and purges indicated that a negligible amount (∿0.1%) of tritium was sorbed on the system surfaces.

The release of krypton from the coprecipitated $(U,Pu)O_2$ during the heat-up period of the 600°C experiment was about 6% of the total fuel content (FBR-4). Krypton release from the mechanically blended fuel during the same period for the 650°C experiments was approximately the same, 9% and 6%, respectively, for FBR-1 and FBR-2. Concentration of ^{85}Kr in the off-gas rose rapidly during the first 30 min the fuel was at temperature and followed the shape of the oxygen consumption curve. Evolution rates then decreased gradually, taking up to two or more hours for the remainder of the released ^{85}Kr to be collected. Sweep-out time for the system at 300 cm^3/min was about 10 min.

3.2.4 Rate of oxygen consumption

The combined profiles for oxygen consumption and gaseous fission product release during the FBR-4 voloxidation at 600°C were shown in the previous section.

During the heat-up period in both experiments with coprecipitated fuel, the oxygen consumption was apparently minimal until the temperature of the charge had reached about 600°C. Oxidation began at temperatures in the 400 to 450°C range during the runs with mechanically blended $(U,Pu)O_2$.[2] In all experiments, maximum consumption was reached within 15 min of the time the voloxidation temperature (600 or 650°C) was reached. The peak consumption during the 600°C run occurred with a broad maximum and about 30% of the oxygen in the feed air stream being consumed. In the 650°C runs, nearly 90% of the input oxygen was being consumed at the peak point in a sharper spike.

3.2.5 Release of gaseous fission products

The inventory of gaseous fission products in the NUMEC mechanically blended and coprecipitated mixed oxide was determined by dissolution of voloxidized and nonvoloxidized fuel samples and from the collected voloxidizer and dissolution off-gases. They are shown in Table 5 for each rod as mean values from four experimental determinations.

Table 5. Gaseous radionuclide inventories in NUMEC $(U,Pu)O_2$

Rod No.	Gaseous fission product content [dis sec^{-1} $g(U + Pu)^{-1}$][a]		
	^3H	^{14}C	^{85}Kr
B-7	1.01×10^5	4.52×10^4	5.58×10^7
C-13	1.51×10^5	4.41×10^4	8.88×10^7

[a]Four experimental determinations

Voloxidations performed in air at 600 and 650°C resulted in the release of appreciable amounts of the ^3H, ^{14}C, and ^{85}Kr from the fuel. These are presented in Table 6, listed as percent of the total fuel inventories given in Table 5.

Table 6. Release of gaseous radionuclides during voloxidation of NUMEC $(U,Pu)O_2$

Run No.	Rod No.	Fuel type[a]	Voloxidation temperature (°C)	Released to voloxidizer off-gas (% of total fuel inventory)		
				^3H[b]	^{14}C[b]	^{85}Kr[c]
FBR-1	B-7	MB	650	95.9	87.3	38.2
FBR-3	B-7	CP	600	99.0	97.9	13.1[d]
FBR-2	C-13	MB	650	91.5	66.4	52.6
FBR-4	C-13	CP	600	98.2	76.9	56.5

[a]MB, mechanically blended; CP, coprecipitated.

[b]Based on residual levels determined from dissolution of voloxidized oxide.

[c]Determined from collected voloxidizer off-gas.

[d]Gas collection for only the first 20 min at voloxidation temperature.

Tritium releases were generally greater than 95%. The average release was slightly greater at 600°C than at 650°C. However, from data presented earlier,[2] the mechanically blended samples voloxidized at 650°C also contained greater amounts of tritium prior to voloxidation (due to probable contamination from axial-blanket UO_2 during shearing and sample preparation). In two experiments, the amount of tritium recovered from the voloxidizer off-gas by silica gel traps was essentially 100% of the amounts listed in Table 5.

Releases of the ^{14}C from the fuel were relatively large, and the average evolution also tended to be slightly higher (by ∿10%) in the 600°C voloxidation experiments than at 650°C.

Total ^{85}Kr release figures at 600°C for the B-7 rod (run No. FBR-3) were obscured by an interruption in the gas collection during the experiment; however, the amount released within the first 20 min at 600°C was about one-third the amount of ^{85}Kr released at 650°C. For the coprecipitated portion of the C-13 rod, there appeared to be no significant variation in the release of ^{85}Kr from that of the mechanically blended oxide.

3.2.6 Fission product distribution during voloxidation

The inventories of selected fission products in each of the NUMEC rods are listed in Table 7. Recoveries (as percentages of these amounts) are shown for rods B-7 and C-13 in Tables 8 and 9, respectively. Detection limits on the method of gamma spectrometry used to analyze samples from FBR-1 prevented complete analysis of ^{106}Ru, ^{125}Sb, and ^{144}Ce due to decay and masking by the high levels of ^{137}Cs activity. The results for the fission product distributions in the off-gas system during run FBR-3 are incomplete because the filter trap and heated lines were disconnected after the first 20 min at 600°C; however, the deposition tubing samples remained in place for the entire run.

Less than 1.0% of the total ^{106}Ru, ^{125}Sb, and ^{144}Ce was released from the fuel and was found in the system after voloxidation at either 600 or 650°C. The amounts of $^{134-137}Cs$ volatilized ranged from 4 to 6% of the totals in the fuel for both rods. Approximately two to three times more cesium was found deposited within the voloxidizer than in off-gas sample locations. Results from one experiment at 650°C indicated

Table 7. Inventories of selected fission products found in NUMEC $(U,Pu)O_2$

	Fission product content [dis sec^{-1} $g(U + Pu)^{-1}$]^a					
	^{106}Ru	^{125}Sb	^{129}I	^{134}Cs	^{137}Cs	^{144}Ce
B-7	1.34×10^9	4.44×10^8	220[b]	2.55×10^8	1.13×10^{10}	3.10×10^9
C-13	1.40×10^9	5.77×10^8	220[b,c]	3.89×10^8	1.17×10^{10}	3.05×10^9

[a]Four experimental determinations.

[b]μg/g.

[c]Assumed B-7 content as best value.

Table 8. Selected fission product recoveries from the voloxidizer and off-gas system following voloxidation of $(U,Pu)O_2$ from NUMEC rod B-7

Nuclide	Run No.	Voloxidizer temperature (°C)	Distribution (% of fuel inventory)	
			Voloxidizer walls	Off-gas system
^{106}Ru	FBR-1	650	a	a
	FBR-3	600	0.51	0.03[b]
^{125}Sb	FBR-1	650	a	a
	FBR-3	600	0.88	0.002[b]
^{129}I	FBR-1	650	0.77	80.82
	FBR-3	600	2.67	25.77[b]
^{134}Cs	FBR-1	650	4.35	1.61
	FBR-3	600	4.16	2.02[b]
^{137}Cs	FBR-1	650	2.88	0.66
	FBR-3	600	3.39	1.66[b]
^{144}Ce	FBR-1	650	a	a
	FBR-3	600	0.12	0.003[b]

[a]Below detection limits, or <<0.001%.

[b]Off-gas system disconnected after initial 20 min at 600°C during FBR-3.

Table 9. Selected fission product recoveries from the voloxidizer and off-gas system following voloxidation of $(U,Pu)O_2$ from NUMEC rod C-13

Nuclide	Run No.	Voloxidizer temperature (°C)	Distribution (% of fuel inventory) Voloxidizer walls	Off-gas system
^{106}Ru	FBR-2	650	0.07	0.04
	FBR-4	600	0.31	0.13
^{125}Sb	FBR-2	650	0.11	0.08
	FBR-4	600	0.80	a
^{129}I	FBR-2	650	0.80	75.73
	FBR-4	600	3.96	41.14
^{134}Cs	FBR-2	650	2.96	1.48
	FBR-4	600	3.57	1.48
^{137}Cs	FBR-2	650	2.88	1.26
	FBR-4	600	3.08	1.49
^{144}Ce	FBR-2	650	0.19	0.05
	FBR-4	600	0.21	0.04

[a]Not detected.

only about 0.66% of the ^{137}Cs in the fuel was transferred to the off-gas system. However, recoveries on deposition tubing and filter samples during this run seem low when compared to those from other experiments where they ranged from 1 to 2% of the total ^{137}Cs inventories. Surprisingly, in almost every case,more fission products were found deposited on the surfaces or in the traps following the 600°C experiments than after the 650°C tests (this is discussed in Sect. 3.2.7); the exception was ^{129}I. Although more ^{129}I was recovered from the voloxidizer walls after the 600°C runs, less of the total ^{129}I in the fuel was apparently volatilized, because recoveries on the downstream heated charcoal beds at 125°C were significantly less than during the 650°C voloxidations.

Distributions of fission products in the off-gas system following voloxidations of fuel from rods B-7 and C-13 are shown in Tables 10 and 11, respectively. Most of the fission products that passed the 35-μm pore-size gas exit of the voloxidizer were found on stainless steel tubing insert specimens. In the three runs in which the off-gas was filtered

Table 10. Distribution of selected fission products remaining in the voloxidizer off-gas system following oxidation of $(U,Pu)O_2$ from NUMEC Rod B-7

Nuclide	Voloxidation temperature (°C)	System distribution (% of total released from voloxidizer)							Total found in off-gas system [dis sec^{-1} g(U + Pu)$^{-1}$
		Deposition tubing[a]	Graded filter papers ≥ 5 μm	Graded filter papers 0.3 μm	Charcoal bed	Ag-zeolite pellets	Off-gas line	HEPA filter	
^{106}Ru	650							b	
	600	89.9					10.14	0	3.72×10^5
^{129}I	650	7.4	0.05	b	86.8	7.42	<<0.01	b	177.8[c]
	600	97.7	0.43	0.18	1.68	c	d	e	56.7[c]
^{134}Cs	650	92.2	1.07	b	3.76	2.73	0.24	b	9.11×10^6
	600	97.4	0.05	0.06	0.03	c	2.50	0.01	5.14×10^6
^{137}Cs	650	92.4	1.05	b	3.75	2.58	0.25	b	1.97×10^8
	600	99.1	0.04	0.06	0.03	b	0.78	<0.01	1.88×10^8

[a]During the 600°C run, the off-gas line following the deposition tubes was disconnected after 20 min of operation.

[b]Does not apply.

[c]μg/g.

[d]Not detected by activation analysis for iodine.

Table 11. Distribution of selected fission products remaining in the voloxidizer off-gas system following oxidation of $(U,Pu)O_2$ from NUMEC rod C-13

Nuclide	Temp (°C)	System distribution (% of total released from voloxidizer)						Total found in off-gas system [dis sec^{-1} $g(U + Pu)^{-1}$]
		Deposition tubing	Graded filter papers ≤ 0.5 μm	Graded filter papers 0.3 μm	Charcoal bed	Off-gas line	HEPA filter	
^{106}Ru	650	82.6	1.25	14.60	0.25	0.08	1.25	6.29×10^5
	600	93.3	1.42	1.08	0.25	3.44	0.52	1.80×10^6
^{129}I	650	1.9	0.29	0.73	97.00	<< 0.01	0.3	166.6[a]
	600	0.4	b	b	99.60	b	b	90.5[a]
^{134}Cs	650	81.1	1.41	15.50	0.40	0.40	1.21	5.74×10^6
	600	89.1	3.08	2.49	0.49	2.93	1.88	5.74×10^6
^{137}Cs	650	81.4	1.36	15.50	0.34	0.35	1.08	1.48×10^8
	600	89.3	3.26	2.63	0.52	2.37	1.88	1.74×10^8
^{144}Ce	650	74.2	1.79	21.60	0.41	0.41	1.66	1.41×10^6
	600	90.8	1.85	1.74	0.26	4.73	0.65	1.15×10^6

[a] μg/g.

[b] Not detected.

and sampled for the entire experiment, the largest percentage of recovered ^{129}I was on the heated charcoal beds. Iodine collected on filter papers and charcoal during the initial 20 min of the FBR-3 voloxidation at 600°C amounted to about 0.6% of the total ^{129}I in the fuel.

Profiles of the fission product deposition from the voloxidizer off-gas onto cooler surfaces are shown in Figs. 5 and 6 for runs FBR-3 and FBR-4 respectively. The results are almost identical for both runs. Deposition profiles for the 650°C experiments were reported previously.[2] Except for ruthenium, the deposition patterns appeared similar for voloxidations at both temperatures. Ruthenium did not volatilize as much at 650°C as at 600°C. This phenomenon is also evident in ratios of fission product quantities sampled from the voloxidizer system (Table 12). A comparison of the fission product ratios at the various sample locations in the off-gas system and the fission product ratios determined for the original fuel indicate that most of the fission products were truly volatilized instead of transported as particles of fuel. During both runs at 600°C, increased concentrations of ^{106}Ru were measured on the cooler end of the tubing specimens, possibly signifying some region (near 225°C) at which enhanced collection of volatilized ruthenium from this fuel might exist under these conditions. As part of another investigation on deposition and scouring of ruthenium oxides,[4] increased RuO_2 deposition on stainless steel substrates has been measured at temperatures in the range 450 to 550°C and also at about 250°C. This was thought to be related to an enhancement of the self-catalyzed RuO_4 decomposition process occurring in these two temperature regions.

Most of the entrained activity found on graded filters in the 650°C experiments was associated with particulates sized between 0.3 and 5 μm. There was less recovery of particulate-type activity following the 600°C runs. The slightly larger amounts of fission products were found on the heated off-gas lines following runs FBR-3 and FBR-4. This is probably due to the use of more concentrated nitric acid leach solutions than had been used after the 650°C runs. Only small quantities of radionuclides were carried by the off-gas to HEPA filters located outside the cell.

3.2.7 Discussion of voloxidation results

Much thermogravimetric analysis data have been reported[5] on the oxidation of unirradiated NUMEC coprecipitated and mechanically blended $(U_{0.8}Pu_{0.2})O_2$ archive pellets. In these studies, the coprecipitated

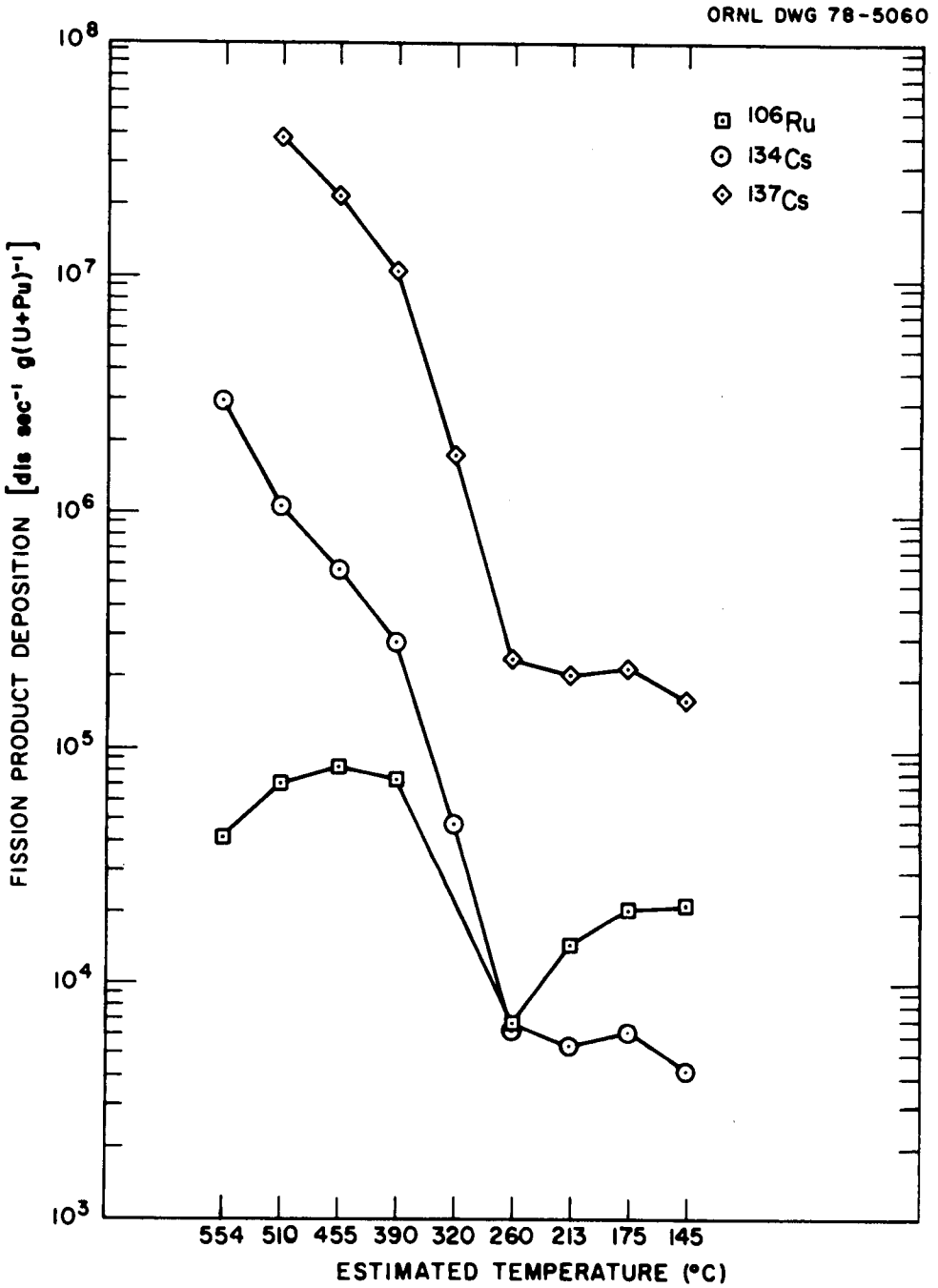

Fig. 5. Fission product deposition from voloxidizer off-gas (FBR-3).

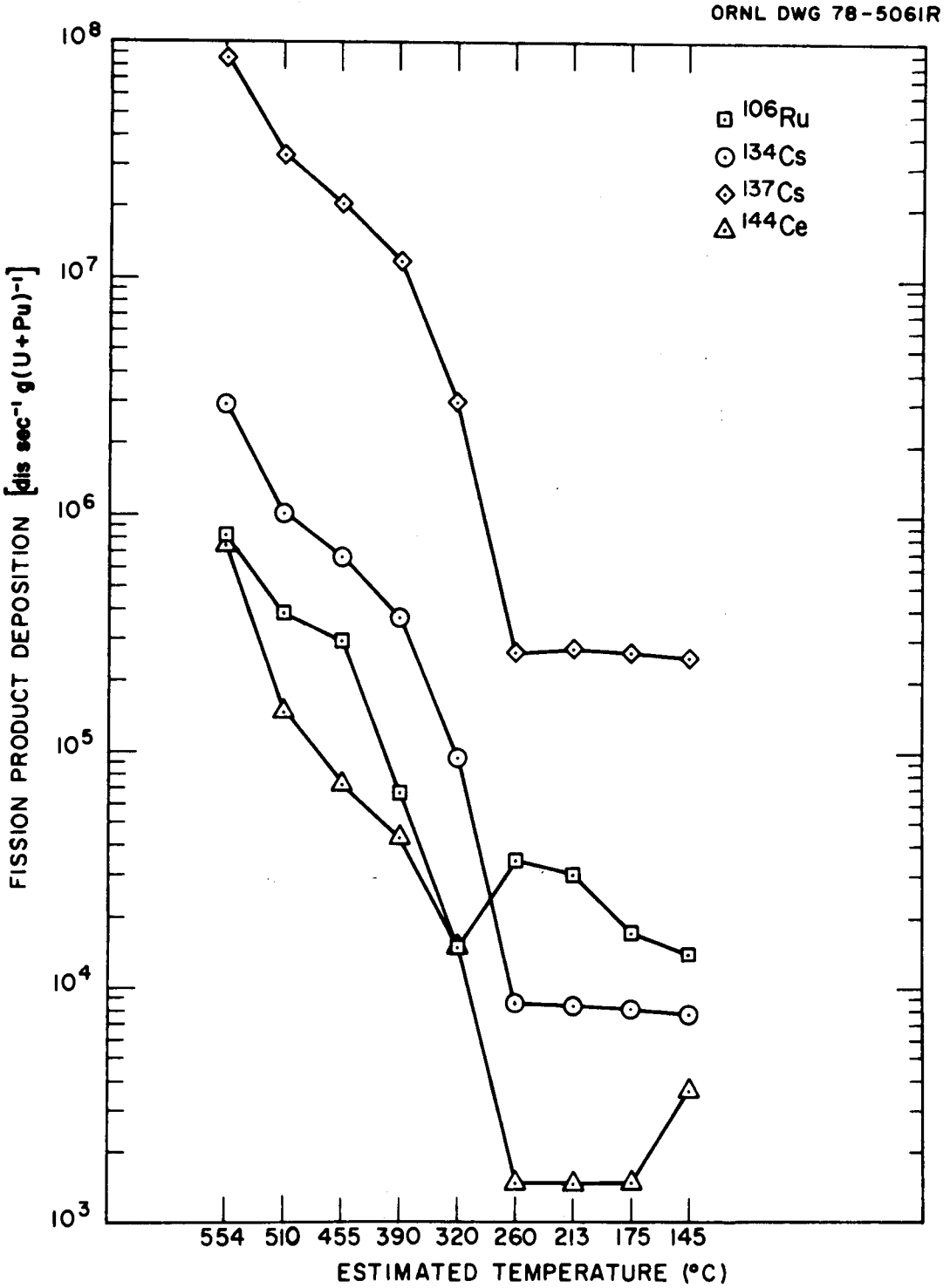

Fig. 6. Fission product deposition from voloxidizer off-gas (FBR-4).

Table 12. Ratios of selected fission products recovered from the voloxidizer and off-gas system following oxidation of $(U,Pu)O_2$ from NUMEC rod C-13

Nuclide ratio	Voloxidation temperature (°C)	Sample system location					
		Fuel[a]	Voloxidizer walls	Deposition tubing (high temp)[b]	Deposition tubing (low temp)[b]	Filter papers ($\geq$ 0.3 μm)	Off-gas system[c]
$^{106}Ru/^{137}Cs$	600	0.120	0.012	0.011	0.113	0.004	0.010
	650	0.120	0.003	0.006	0.005	0.025	0.004
$^{134}Cs/^{137}Cs$	600	0.033	0.039	0.031	0.031	0.031	0.033
	650	0.033	0.032	0.040	0.040	0.039	0.039
$^{106}Ru/^{144}Ce$	600	0.460	0.706	2.20	18.80	1.00	1.43
	650	0.460	0.188	0.75	0.25	1.92	0.400
$^{134}Cs/^{144}Ce$	600	0.128	2.45	6.80	5.71	7.86	4.99
	650	0.128	1.98	4.90	2.04	2.91	4.07
$^{137}Cs/^{144}Ce$	600	3.83	58.8	200.0	166.7	250.0	142.8
	650	3.83	62.5	125.0	50.0	76.9	100.0

[a]Based on experimentally determined inventories.

[b]High-temperature region, ∿525°C; low-temperature region, ∿225°C.

[c]Includes deposition tubing, filters, charcoal, and heated lines.

pellets were from NUMEC fabrication batches 5 and 6, whereas the irradiated pellets in these experiments were from batch 4. The unirradiated, mechanically blended pellets were from batch 16, and the irradiated pellets were part of batch 15.

Tennery reported that complete oxidation to an oxygen-to-metal (O:M) ratio of 2.55 took place in two stages within a narrow temperature range of 500 to 600°C. This produced a theoretical weight gain of about 3.3%. Over a wider range of temperatures, the first stage (O:M ratio = 2.35) was easily reached; this corresponded to the M_3O_7 phase [i.e., $(U_{2.4}Pu_{0.6})O_2$ and about a 2% weight gain]. The second stage, conversion to U_3O_8 + PuO_2 (weight gain, 3.3%, O:M = 2.55) was more difficult and could not be reached at temperatures above 600°C. In ref. 5, Fitzgerald and Farrar reported maximum weight gains of 2.2 to 2.4% at 450°C, and 2.5 to 2.7% at 650°C; these values correspond to 71 to 76% and 80 to 84% conversion of the UO_2 in the mixed oxide to U_3O_8; Haire et al. reported similar results.

Studies made with unirradiated archive $(U,Pu)O_2$ pellets under closely controlled conditions in glove boxes indicated that only partial oxidation of the irradiated mixed oxide would probably take place (i.e., from an O:M ratio of about 1.98 to 1.99 to 2.35, or a weight gain of about 2.5%). For a 31.5-g batch of irradiated fuel (e.g., run FBR-2), the theoretical increase in weight should be about 0.8 g. We conclude that the oxidation of irradiated NUMEC coprecipitated fuels at 600°C was probably more complete than the oxidation of mechanically blended fuels at 650°C.

The greater release of fission products from the fuel at 600 than at 650°C may be explained by the work of Tennery.[5] At 650°C, the oxidation of the $(U,Pu)O_2$ does not go to completion but stops at an O:M ratio of about 2.35. The phase boundary at O:M = 2.55 that causes disintegration of the fuel is therefore not crossed; consequently, fewer of the fission products in the fuel matrix are exposed.

3.3 Dissolution Studies

3.3.1 Leaching procedure

Leaching the as-sheared or voloxidized fuel was conducted in the following sequence for all samples:

DS-1: 2 hr, 8 M HNO_3, 92 to 95°C. Cool, centrifuge solution, decant, rinse solids, analyze solution.

DS-2: 2 hr, 3 M HNO_3, 92 to 95°C. Cool, centrifuge solution, decant, analyze solution.

DS-3: 2 hr, 8 M HNO_3, 92 to 95°C. Cool, centrifuge solution, decant, analyze solution.

DS-4: 2 hr, 8 M HNO_3--0.05 M KF, 92 to 95°C (for material balance purposes on plutonium).

After the leaches, the insoluble residue was separated from the cladding, dried, weighed, and analyzed. The stainless steel cladding was also dissolved in 5 M HNO_3--2 M HCl--0.05 M KF to determine residual actinide and fission product contents.

3.3.2 Material balances

Material balances, based on weights, were made for the dissolution experiments (Table 13). In almost all cases, results were within the accuracy of our weighing capability (± 0.1 g) and the analyses for uranium and plutonium (± 3%), and fission products (± 5%).

3.3.3 Solubility of uranium and plutonium

The dissolution results for the coprecipitated and mechanically blended fuels are summarized in Tables 14 and 15. Essentially no uranium was found in the insoluble residues. Plutonium losses (with the exception of run 3A, Table 14) ranged from about 0.02 to 0.68% with unvoloxidized fuel to 1.14 to 2.21% with voloxidized fuel. More than 96% of the plutonium dissolved in the first 2 hr; the 3 and 8 M HNO_3 leaches slowly dissolved the rest of the soluble plutonium. In many cases, the cladding contained small amounts of fissile material; the larger amounts (e.g., run FBR-3A) may have been caused by physical entrapment of fuel by the sheared metal or by an external source of contamination. Voloxidation appeared to increase the amount of plutonium associated with the cladding. The fabrication route of the fuel apparently had little effect on the solubility.

3.3.4 Ionic analyses of NUMEC dissolver solutions

Table 16 shows the results of spark-source mass spectrometry (SSMS) of four different dissolver solutions , and gives the concentrations of soluble fission and corrosion products had been dissolved with the uranium and plutonium. The final nitric acid concentrations in the solutions were 4.1 to 4.7 M HNO_3.

Table 13. Material balances for dissolution experiments with NUMEC fuel rods

Exp. No.	NUMEC rod	Fuel type[a]	No. pieces	Starting wt (g)	Leached clad (g)	$(U,Pu)O_2$ by analysis (g)	Total residue (g)	Soluble fission products[b] (g)	Total recovered (g)	Difference (%)
1A	B-7	MB	2	5.9	1.41	4.33	0.05	0.21	6.00	+1.7
1BC	B-7	MB	11	40.9	8.50	30.10	0.50	1.36	40.46	-1.1
2A	C-13	MB	1	6.8	1.52	4.77	0.06	0.23	6.58	-3.2
2B	C-13	MB	11	40.1	8.74	28.82	0.58	1.58	39.72	-0.9
3A	B-7	CP	2	5.9	1.52	4.26	0.06	0.20	6.04	+2.4
3B	B-7	CP	14	44.9	9.60	32.24	0.84	1.52	44.20	-1.6
4A	C-13	CP	2	5.8	1.58	3.58	0.07	0.19	5.42	-6.6
4B	C-13	CP	13	43.0	8.10	30.21	1.31	1.66	41.28	-4.0

[a]MB = mechanically blended; CP = coprecipitated.

[b]Estimated from spark source mass spectrometry data.

Table 14. Dissolution of NUMEC coprecipitated $(U,Pu)O_2$

Analysis	Not voloxidized; % total dissolved				Voloxidized at 600°C; % total dissolved			
	Rod No. B-7, run No.3A		Rod No. C-13, run No. 4A		Rod No. B-7, run No. 3B		Rod No. C-13, run No. 4B	
	U	Pu	U	Pu	U	Pu	U	Pu
DS-1	97.89	97.91	99.59	99.18	99.28	96.94	97.98	97.37
DS-2	0.02	0.05	0.05	0.10	0.46	0.41	1.94	1.02
DS-3	0.03	0.05	0.01	0.04	0.11	0.63	0.04	0.46
DS-4	0.02	0.03	0.01	0.01	0.13	1.83	0.03	0.85
Cladding	1.90[a]	1.95[a]	0.004	<0.001	0.02	0.13	<0.001	0.206
Residue	0.13	<0.01	0.31	0.67	0.01	0.06	0.01	0.08

[a]Possibly externally contaminated; appeared when leached cladding was dissolved in aqua regia, but not in the previous HNO_3-KF leach of cladding plus residue (DS-4).

Table 15. Dissolution of NUMEC mechanically blended $(U,Pu)O_2$

Analysis	Not oxidized; % total dissolved				Oxidized at 650°C; % total dissolved			
	Rod No. B-7, run No. 1A		Rod No. C-13, run No. 2A		Rod No. B-7, run No. 1BC		Rod No. C-13; run No. 2B	
	U	Pu	U	Pu	U	Pu	U	Pu
DS-1	99.72	99.78	99.79	99.55	99.27	97.32	99.00	96.32
DS-2	0.11	0.09	0.12	0.38	0.36	0.45	0.60	0.81
DS-3	0.14	0.12	0.06	0.04	0.16	0.58	0.17	0.67
DS-4	0.02	<0.01	0.01	0.01	0.09	1.57	0.12	2.13
Cladding	0.01	0.01	<0.01	<0.01	0.06	0.02	0.09	0.02
Residue	<0.01	<0.01	0.02	0.01	0.05	0.06	0.03	0.06

Table 16. Spark-source mass spectrometric analysis

Element	μg/g Uranium	Element	μg/g Uranium
Ba	5.0	Pd	5.0
Ce	4.9	Pm	1.1
Cs	12.6	Pr	2.7
Cr	0.5	Rb	2.1
Dy	2.0	Sb	1.7
Eu	0.4	Sm	4.4
Fe	3.1	Sr	4.1
La	2.7	Tc	3.1
Mo	6.3	Te	3.2
Nd	16.5	Y	1.2
Ni	0.6	Zr	4.9

3.3.5 Dissolution residues

It was indicated in the overall dissolution material balances (Table 13) that voloxidation increased the weight of insoluble residue after dissolution. Table 17 more fully describes the residues and indicates that the mechanically blended portions of the rods generated less residue than the coprecipitated portions of the same rod, and that voloxidation increased the amount of residue from both types of fuel.

A partial explanation for the differences within a single rod may lie in the variation in burnup along the length of the $(U,Pu)O_2$ in each rod as a function of the height of the 14.5-in.-high core of the EBR-2. The fission rate varies greatly along the length of a fuel rod, and thus creates different burnups within the same rod (Figs. 7 and 8). A rough calculation based on the fission rate curves in Fig. 7 or 8 indicates that the burnup of the coprecipitated (lower) portion of each rod was a factor of about 1.5 greater than the mechanically blended upper portion. The UO_2 blankets would also undergo much less fission than the $(U,Pu)O_2$ fuel in the NUMEC rods.

Table 17. Residues from dissolution of NUMEC $(U,Pu)O_2$

Run No.	NUMEC rod	Fuel type[a]	Voloxidized	$(U,Pu)O_2$ by analysis (g)	Dissolution residue	
					g	%
1A	B-7	MB	No	4.33	0.0494	1.14
1BC	B-7	MB	Yes	30.10	0.5027	1.67
2A	C-13	MB	No	4.77	0.0552	1.16
2B	C-13	MB	Yes	28.82	0.5848	2.03
3A	B-7	CP	No	4.26	0.0614	1.44
3B	B-7	CP	Yes	32.24	0.8377	2.60
4A	C-13	CP	No	3.58	0.0729	2.04
4B	C-13	CP	Yes	30.21	1.3125	4.39

[a]MB = mechanically blended $(U,Pu)O_2$; CP = coprecipitated $(U,Pu)O_2$.

Analysis of the dissolution data also indicated that voloxidation caused a marked difference in the ratio of Pu/(U + Pu) in the nitric acid-insoluble residues:

	Mechanically blended	Coprecipitated
Not voloxidized	0.104	0.224
Voloxidized	0.579	0.819

Since the ratio of Pu/(U + Pu) from the unvoloxidized fuel is roughly similar to the original composition, the change suggests the possibility that voloxidation might break down the UO_2-PuO_2 solid solution structure to form PuO_2-rich crystallites.

Spark-source mass spectrometry and emission spectroscopy showed the primary constituents of the residues were: 10 to 20 wt % rhodium, 20 to 45 wt % ruthenium, 5 to 15 wt % molybdenum; 4 to 20 wt % technetium, 3 to 14 wt % iron, 3 to 7.5 wt % palladium, and up to 4 wt % chromium.

3.3.6 Isotopic composition of NUMEC fuel rods

Figures 7 and 8 also summarize the mass spectrometric determinations of the plutonium and uranium isotopes along the length of NUMEC rods B-7 and C-13, which had nominal 16.5 and 17.5 at. % burnups respectively. [The uranium in the $(U,Pu)O_2$ had been initially enriched to 93% ^{235}U; the

ORNL DWG 78-449R

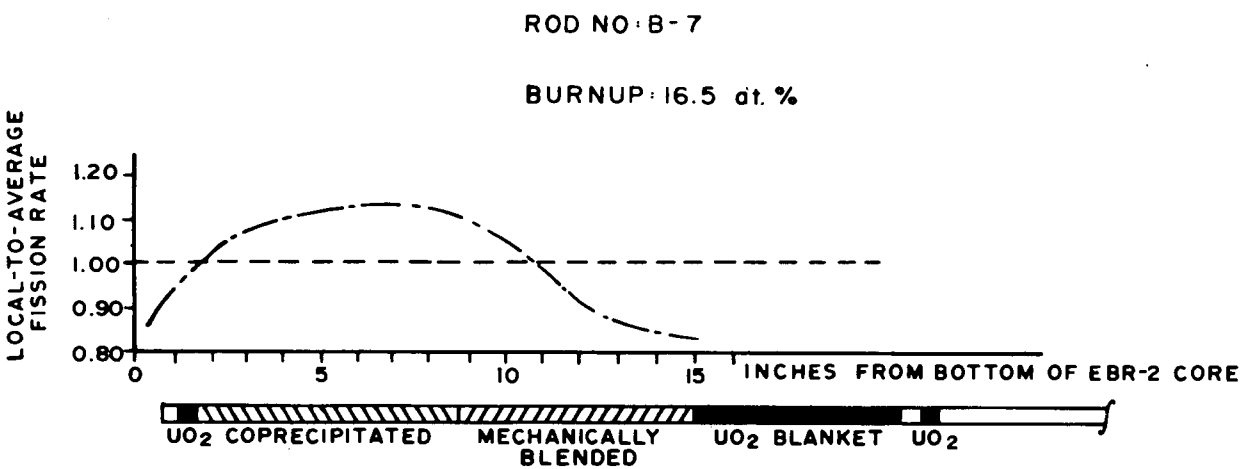

	ATOM %	ATOM %	ATOM %	ATOM %
^{233}U	<0.001	<0.001	<0.001	<0.001
^{234}U	0.642	0.667	0.029	0.005
^{235}U	89.90	89.29	4.099[a]	0.703
^{236}U	2.918	2.97	0.153	0.032
^{238}U	6.539	7.08	95.69	99.26
^{238}Pu	0.023	0.042	0.049	NO ANALYSIS
^{239}Pu	91.350	91.13	94.75	
^{240}Pu	8.225	8.41	4.92	
^{241}Pu	0.368	0.380	0.273	
^{242}Pu	0.029	0.031	0.013	

[a]PROBABLE CONTAMINATION BY ENRICHED URANIUM FROM MIXED OXIDE

Fig. 7. Postirradiation isotopic analysis of NUMEC $(U,Pu)O_2$ rods irradiated in EBR-2 (rod B-7).

ORNL DWG 78-448A

ROD NO. C-13

BURNUP: 17.5 at. %

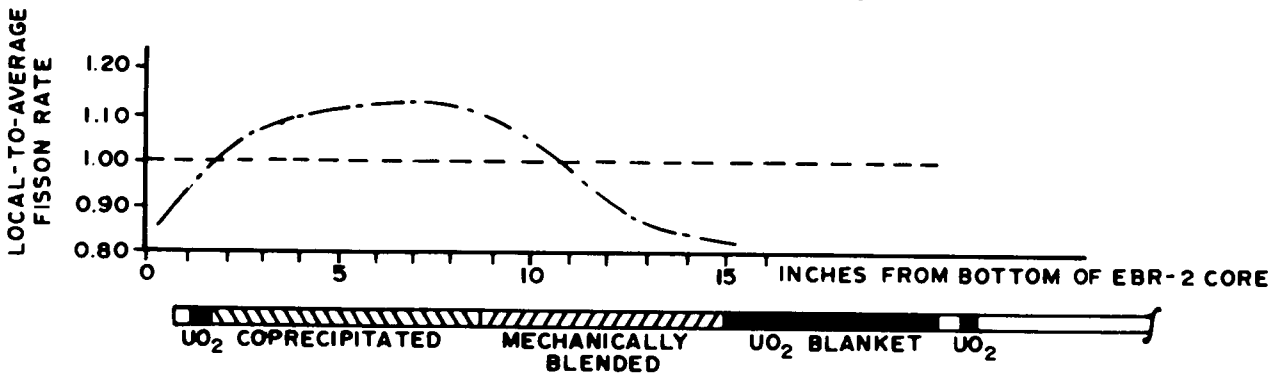

	ATOM %	ATOM %	ATOM %	ATOM %
^{233}U	< 0.001	<0.001	<0.001	<0.001
^{234}U	0.680	0.674	0.006	0.005
^{235}U	87.093	88.920	0.763	0.902
^{236}U	3.592	3.450	0.034	0.052
^{238}U	8.637	7.462	99.197	99.039
^{238}Pu	0.032	0.029	0.027	NO ANALYSIS
^{239}Pu	90.456	90.67	97.10	
^{240}Pu	9.063	8.99	2.751	
^{241}Pu	0.412	0.403	0.115	
^{242}Pu	0.033	0.033	0.008	

Fig. 8. Postirradiation isotopic analysis of NUMEC $(U,Pu)O_2$ irradiated in EBR-2 (rod C-13).

UO_2 blankets contained normal uranium.] Some cross-over, due to the difficulty of locating the exact interface between the enriched uranium fuel and the "normal" uranium blanket, occurred with rod B-7 during shearing and appeared as about 4% ^{235}U in the UO_2 blanket. The burnups of portions of the blanket UO_2 used in the dissolutions were 0.31 and 0.57 at. %, based on the ^{144}Ce content of each.

3.3.7 Stability of dissolver solutions

Results of studies within another ORNL program[6] indicated that a slow agglomeration and settling of colloidal noble-metal fission product particles occurs after an initial clarification of dissolver solutions. We attempted to determine the composition of the solids that were centrifuged from two previously clarified, aged dissolver solutions. A reasonable material balance was obtained for the solids settling out of the solution from rod B-7 (run 3B), but not for run 4B (rod C-13). The secondary precipitate in run FBR-3B (Table 18) appeared to be principally corrosion products from the cladding plus small amounts of $(Pu,U)O_2$ having a Pu/(U + Pu) ratio (0.72) similar to that of the residue from the original dissolution (0.58). The precipitate from the other run (FBR-4B) was much heavier, but contained less uranium and plutonium. The principal components in the FBR-4B residue (identified by SSMS) were inert elements, noble-metal fission products, and corrosion products.

3.3.8 Fission product content of NUMEC rods

The mean values (where possible) of the nuclides in NUMEC rods B-7 and C-13 were calculated for the mixed oxide and axial blanket portions of each rod (Table 19). These values supplement the postirradiation isotopic analyses for the uranium and plutonium and provide a basis for calculation of concentrations in feed solutions, etc. The results clearly show the movement of the gaseous precursor of ^{134}Cs, since the low burnup UO_2 in the blanket contained as much or more than the higher burnup $(U,Pu)O_2$ fuel section.

The estimated fission product content of the two rods was calculated using the ORIGEN[3] computer code. The calculated and analytically determined values for some of the major fission products are listed in Table 20. Reasonable agreement was found for the nonvolatile elements, although many of the analytical values were greater than the calculated values. This was

Table 18. Stability of aged solutions of dissolved, voloxidized coprecipitated $(U,Pu)O_2$

Run No.	FBR-3B	FBR-4B
Original $(U,Pu)O_2$ dissolved, g	32.24	3.56
Concentration of (U + Pu), mg/ml	220.82	48.25
HNO_3 Concentration, M	4.06	6.73
Weight dissolution residue, g	0.838	0.073
Days aged after first clarification	62	82
Weight of secondary ppt, g	0.0022	0.0466
Secondary ppt composition, mg		
U[a]	0.042	0.003
Pu[a]	0.106	0.031
Te[b]	0.088	<1
Ru[b]	0.220	4.660
Fe[b]	1.540	0.690
Mn[b]	0.013	0.186
Cr[b]	0.088	0.466
	2.097	6.036

[a]Chemical analysis.

[b]SSMS analysis.

Table 19. Concentrations of nuclides recovered by dissolution of irradiated NUMEC fuel rods

Nuclide	Rod B-7		Rod C-13	
	Fuel[a]	Blanket[b]	Fuel[a]	Blanket[b]
Burnup, at. %	16.5	0.57	17.5	0.31
Pu/(U + Pu) ratio	0.188	0.018	0.185	0.015
Pu α, counts min^{-1} (mg Pu)$^{-1}$	$9.23 \pm 0.24 \times 10^{7}$	8.88×10^{7}	$9.31 \pm 0.05 \times 10^{7}$	8.02×10^{7}
Pu α, counts min^{-1} [g(U + Pu)]$^{-1}$	$1.74 \pm 0.07 \times 10^{10}$	1.56×10^{9}	$1.72 \pm 0.15 \times 10^{10}$	1.12×10^{9}
Gross α, counts min^{-1} [g(U + Pu)]$^{-1}$	$1.89 \pm 0.12 \times 10^{10}$	2.06×10^{9}	$1.98 \pm 0.14 \times 10^{10}$	1.43×10^{9}
$^{3}H_2$, dis sec^{-1} [g(U + Pu)]$^{-1}$[c]	1.01×10^{5}	4.72×10^{5}	1.51×10^{5}	3.93×10^{5}
^{14}C, dis sec^{-1} [g(U + Pu)]$^{-1}$[c]	$4.52 \pm 1.32 \times 10^{4}$	2.41×10^{4}	$4.41 \pm 1.09 \times 10^{4}$	2.64×10^{4}
^{85}Kr, dis sec^{-1} g(U + Pu)]$^{-1}$[c]	5.58×10^{7}	2.31×10^{7}	8.88×10^{7}	3.21×10^{7}
^{99}Tc, μg/g(U + Pu)	3.54×10^{2}		8.13×10^{2}	
^{106}Ru, dis sec^{-1} [g(U + Pu)]$^{-1}$	$1.34 \pm 0.27 \times 10^{9}$	$\leq 1.94 \times 10^{8}$	$1.40 \pm 0.28 \times 10^{9}$	1.24×10^{8}
^{125}Sb, dis sec^{-1} [g(U + Pu)]$^{-1}$	$4.44 \pm 1.83 \times 10^{8}$	$\leq 1.80 \times 10^{7}$	$5.77 \pm 0.68 \times 10^{8}$	1.36×10^{7}
^{129}I, μg/g(U + Pu)	2.20×10^{2}	6	33.9	3.42×10^{2}
^{134}Cs, dis sec^{-1} [g(U + Pu)]$^{-1}$	$2.55 \pm 0.98 \times 10^{8}$	3.88×10^{8}	$3.89 \pm 1.43 \times 10^{8}$	3.78×10^{8}
^{137}Cs, dis sec^{-1} [g(U + Pu)]$^{-1}$	$1.13 \pm 0.35 \times 10^{10}$	3.32×10^{9}	$1.17 \pm 0.43 \times 10^{10}$	4.12×10^{8}
^{144}Ce, dis sec^{-1} [g(U + Pu)]$^{-1}$	$3.10 \pm 0.20 \times 10^{9}$	2.22×10^{8}	$3.05 \pm 0.33 \times 10^{9}$	1.13×10^{8}

[a]Four experiments.

[b]One experiment.

[c]As of June 1, 1977 (1440 days decay).

Table 20. Comparison of calculated and experimental inventories of fission products in two NUMEC rods

Nuclide	Calculated value (dis sec^{-1} g^{-1})		C-13/B-7 ratio	Experimental value (dis sec^{-1} g^{-1})[a]		C-13/B-7 ratio
	Rod B-7	Rod C-13		Rod B-7	Rod C-13	
$^{3}H_2$	6.92×10^{7}	8.03×10^{7}	1.16	1.01×10^{5}	1.51×10^{5}	1.50
^{14}C	7.81×10^{4}	9.34×10^{4}	1.20	4.52×10^{4}	4.41×10^{4}	0.98
^{85}Kr	9.14×10^{8}	1.06×10^{9}	1.16	5.58×10^{7}	8.88×10^{7}	1.51
^{99}Tc[b]	2.69×10^{3}	3.17×10^{3}	1.18	3.54×10^{2}	8.13×10^{2}	2.30[c]
^{106}Ru	1.20×10^{9}	1.23×10^{9}	1.03	1.34×10^{9}	1.40×10^{9}	1.04
^{125}Sb	3.81×10^{8}	4.18×10^{8}	1.10	4.44×10^{8}	5.77×10^{8}	1.30
^{129}I[b]	6.86×10^{2}	8.09×10^{2}	1.18	2.20×10^{2}	2.20×10^{2}[d]	1.0
^{134}Cs	1.88×10^{8}	2.43×10^{8}	1.29	2.55×10^{8}	3.89×10^{8}	1.53
^{137}Cs	9.66×10^{9}	1.29×10^{10}	1.36	1.13×10^{10}	1.17×10^{10}	1.04
^{144}Ce	2.17×10^{9}	2.04×10^{9}	0.94	3.10×10^{9}	3.05×10^{9}	0.98

[a]Experimental values from Table 15.

[b]μg/g.

[c]Possible incomplete recovery from rod B-7; difficult analysis.

[d]Better value from rod B-7.

probably due to inaccuracies in some of the input data for exact reactor operating conditions. The $^{3}H_2$, ^{14}C, and ^{85}Kr are known to be released from the fuel during irradiation.

3.3.9 Tritium distribution

Experimentally determined concentrations of tritium found in a number of NUMEC experiments irradiated under generally similar conditions in EBR-2 are presented in Table 21. Essentially all (>99.9%) of the tritium from ternary fission had escaped from the mixed oxide fuel through the stainless steel cladding. The tritium in the UO_2 axial blankets did not escape during irradiation, and the concentration was an order of magnitude greater than that in the $(U,Pu)O_2$.

Table 21. Tritium content of NUMEC $(U,Pu)O_2$ irradiated in EBR-2

Rod No.	Burnup (at. %)	Tritium content of (U,Pu)O2 fuel		
		Calculated[a] (dis sec^{-1} g^{-1})	Experimental (dis sec^{-1} g^{-1})	Experimental/calcd ratio (%)
A-8	3.4	3.59×10^7	1.36×10^4	0.038
A-10	3.4	3.59×10^7	1.99×10^4	0.055
B-1	5.3	5.51×10^7	3.48×10^4	0.063
B-7	16.5	6.92×10^7	5.93×10^3[b]	0.086
C-13	17.5	8.03×10^7	6.71×10^3[c]	0.084

[a]Calculated assuming no loss during irradiation.
[b]Tritium content of UO_2 axial blanket 4.67×10^5 dis sec^{-1} g^{-1} uranium.
[c]Tritium content of UO_2 axial blanket 3.88×10^5 dis sec^{-1} g^{-1} uranium.

A material balance for the tritium distribution in the entire NUMEC rod B-7 showed that the 35 g of axial blanket contained 97% of the total tritium in the rod. Analysis of tritium results from rod C-13 were similar (∿96% in the blanket). This suggests that the voloxidation of the mixed core and blanket could occur at 480°C (typical for UO_2 conditions) rather than at 600°C [typical for $(U,Pu)O_2$ conditions]. This might release all of the tritium from the UO_2 and most of the small amount in the mixed oxide. Such tests will be added to the program in the future.

3.3.10 Distribution of fission products during dissolution

The distribution of the fission products during dissolution of the irradiated $(U,Pu)O_2$ fuel is summarized in Tables 22 and 23. The tables are based on the fission products introduced into the dissolver with the fuel; accordingly, the fission product contents of the voloxidized fuel may differ from that of the unvoloxidized material because of the release of portions of the $^{3}H_2$, ^{14}C, ^{85}Kr, and ^{129}I. The data indicate that most of the tritium (90 to 93%) remains in the dissolver solution, while the rest of it appears in the condensate traps and in the caustic scrubber. The ^{14}C is released from the oxide and is trapped in the scrubber. The ^{85}Kr is completely carried out of the dissolver by the off-gas stream. About two-thirds of the ^{129}I was volatilized from the dissolver and was carried to the scrubber; other experiments[6] indicate the iodine can be almost completely volatilized by sparging and chemical treatment.

The other nitric acid-soluble fission products (i.e., $^{134-137}Cs$ and ^{144}Ce) remain in the fuel solution. Voloxidation changes the dissolution behavior of ruthenium and antimony, and (by inference to the insoluble residue above) that of the molybdenum, technetium, and other noble metal fission products. Tables 22 and 23 also show that 10 to 11% of the ^{106}Ru was soluble in the unvoloxidized fuel, but less than 0.5% dissolved after voloxidation. The ^{125}Sb ratio between the fuel solution and residue changed from 97% soluble to only 14% soluble after voloxidation.

4. CONCLUSIONS

Four experiments with unoxidized and four with voloxidized $(U,Pu)O_2$ irradiated to 16.5 to 17.5 at. % burnup in EBR-2 showed:

1. No significant difference in shearing behavior was seen when coprecipitated or mechanically blended pellet rods were cut with a single-pin hydraulic shear. The 17.5-at. % burnup rod released slightly more loose fuel with each cut than the 16.5-at. % rod.
2. Voloxidation of mechanically blended $(U,Pu)O_2$ in air at 12 rpm and 650°C increased the amount of loose fuel in the voloxidizer from 10 to 12% to about 60 to 65% of the total. Voloxidation of coprecipitated $(U,Pu)O_2$ in air at 12 rpm and 600°C increased

Table 22. Distribution of fission products during dissolution of unvoloxidized fuel

Radionuclide	Leach solutions	Insoluble residue	Condensate trap	NaOH scrubber	Off-gas
	(% of total found in dissolution)				
$^{3}H_2$	89.6	<0.1	2.3	7.9	<0.1
^{14}C	2.1	<0.1	<0.1	97.9	<0.1
^{85}Kr	0.0	0.0	0.0	0.0	100
^{106}Ru	10.6	89.4	<0.1	<0.1	<0.1
^{125}Sb	97.5	2.5	<0.1	<0.1	<0.1
^{129}I	32.5	<0.1	1.1	66.5	<0.1
^{134}Cs	99.9	<0.1	<0.1	<0.1	<0.1
^{137}Cs	99.9	<0.1	<0.1	<0.1	<0.1
^{144}Ce	99.9	<0.1	<0.1	<0.1	<0.1

Table 23. Distribution of fission products during dissolution of voloxidized NUMEC fuel[a]

Radionuclide	Leach solutions	Insoluble residue	Condensate trap	NaOH scrubber	Off-gas
	(% of total found in dissolution)				
$^{3}H_2$	92.7	<0.1	1.3	5.8	<0.1
^{14}C	10.3	<0.1	<0.1	89.6	<0.1
^{85}Kr	0.0	0.0	0.0	0.0	100
^{106}Ru	0.4	99.6	<0.1	0.1	<0.1
^{125}Sb	14.3	85.0	<0.1	0.7	<0.1
^{129}I	31.3	<0.1	7.4	61.4	<0.1
^{134}Cs	99.9	<0.1	<0.1	0.1	<0.1
^{137}Cs	99.9	<0.1	<0.1	0.1	<0.1
^{144}Ce	99.9	<0.1	<0.1	0.1	<0.1

[a]Voloxidation releases large fractions of $^{3}H_2$, ^{14}C, ^{85}Kr, and ^{129}I before the dissolution.

the amount of loose fuel to about 83%. In neither case was the product a very fine powder.

3. Voloxidation at 600°C was more effective in releasing $^{3}H_2$, ^{14}C, and ^{85}Kr from the fuel than voloxidation at 650°C. This is presumably due to more complete oxidation (i.e., approaching an O:M ratio of 2.55) at 600°C than at the higher temperature.
4. Tritium releases were generally greater than 95% at both temperatures; ^{14}C releases were 97 to 98% at 600°C and 66 to 87% at 650°C.
5. The ^{85}Kr releases were 38 and 53% at 650°C and 56% at 600°C.
6. The fuel fabrication route apparently did not affect the release of ^{85}Kr or the other gaseous fission products.
7. Less than 1% of the ^{106}Ru, ^{125}Sb, and ^{144}Ce were released at either temperature. Four to six percent of the $^{134-137}Cs$ was released from the fuel, most of which deposited on the walls of the voloxidizer.
8. Up to 80% of the ^{129}I left the voloxidizer at 650°C, with little deposition (<1%) on the internal walls. At 600°C, only 41% was released from the fuel, and most was carried into the off-gas system.

5. ACKNOWLEDGMENTS

We wish to acknowledge the efforts of the skilled Chemical Development Section technicians who performed hot-cell operations: E. C. Hendren, J. R. Travis, and C. S. Webster. Mr. Webster also did a superb job in programming the Hewlett-Packard 3050B on-line data logger and calculation system to record the operating data and calculate and plot the fission product release rates, oxygen consumption, etc. that summarize each voloxidation experiment. J. H. Cooper, J. A. Carter, F. F. Dyer, H. A. Parker, and J. C. Price, ORNL Analytical Chemistry Division, headed their respective service groups who performed the many necessary ionic and radiochemical analyses. V. C. A. Vaughen, Manager, Hot Cell Operations, helped to plan the experiments and reviewed this manuscript.

6. REFERENCES

1. Fabrication of 20 wt % PuO_2-UO_2 Fast Breeder Fuels for Irradiation Testing in EBR-II, NUMEC-3524-74 (June 1970).

2. J. H. Goode and R. G. Stacy, Head-End Processing Studies with Mechanically Blended $(U,Pu)O_2$ Reactor Fuels, ORNL/TM-6266 (in press).

3. M.J. Bell, ORIGEN - The Oak Ridge Isotope Generation and Depletion Code, ORNL-4628 (May 1974)[calculated by R. L. Beatty, U. S. Department of Energy (December 1976)].

4. J. A. Klein, Ruthenium Oxide Deposition and Scouring in a Rotary Kiln Voloxidizer, ORNL/TM-5665 (January 1977).

5. J. H. Goode (ed.), Voloxidation - Removal of Volatile Fission Products from Spent LMFBR Fuels, ORNL/TM-3723 (January 1973).

6. B. L. Vondra, AFCT Program Quarterly Report for Period July 1 to Sept. 30, 1977, ORNL/TM-6076 (November 1977).

ORNL/TM-6370
Dist. Category-79c

Internal Distribution

1. J. T. Bell
2. M. R. Bennett
3. R. E. Blanco
4. J. O. Blomeke
5. W. D. Bond
6. E. C. Bradley
7. R. E. Brooksbank
8-17. W. D. Burch
18. D. D. Cannon
19. J. M. Chandler
20. W. E. Clark
21. J. H. Cooper
22. L. T. Corbin
23. D. A. Costanzo
24. R. M. Counce
25. D. J. Crouse
26. B. F. Crump
27. J. P. Drago
28. M. J. Feldman
29. D. E. Ferguson
30. L. M. Ferris
31-40. J. H. Goode
41. N. R. Grant
42. W. S. Groenier
43. W. R. Hamel
44. D. C. Hampson
45. B. A. Hannaford
46. W. O. Harms
47. R. M. Hill
48. W. D. Holland
49. D. E. Horner
50. A. R. Irvine
51. A. D. Kelmers
52. L. J. King
53. J. Q. Kirkman
54. J. A. Klein
55. C. E. Lamb
56. B. E. Lewis
57. M. H. Lloyd
58. D. K. Lorenzo
59. A. L. Lotts
60. J. C. Mailen
61-63. A. P. Malinauskas
64. D. L. Manning
65. L. Maya
66. A. D. Mitchell
67. J. G. Morgan
66. E. L. Nicholson
69. E. D. North
70. J. H. Pashley
71. F. L. Peishel
72. H. Postma
73. R. H. Rainey
74. J. E. Rushton
75. W. F. Schaffer, Jr.
76. C. D. Scott
77. T. Shapiro
78. B. B. Spencer
79-88. R. G. Stacy
89. J. G. Stradley
90. O. K. Tallent
91. D. B. Trauger
92. W. E. Unger
93-94. V. C. A. Vaughen
95-100. B. L. Vondra
101. B. S. Weil
102. T. D. Welch
103. M. E. Whatley
104. R. G. Wymer
105. O. O. Yarbro
106. S. Beard (Consultant)
107. Manson Benedict (Consultant)
108. L. Burris, Jr. (Consultant)
109. A. B. Carson (Consultant)
110. G. R. Choppin (Consultant)
111. L. J. Colby, Jr. (Consultant)
112. E. L. Gaden, Jr. (Consultant)
113. C. H. Ice (Consultant)
114. W. H. Lewis (Consultant)
115. A. Schneider (Consultant)
116. L. E. Swabb, Jr. (Consultant)
117. M. J. Szulinski (Consultant)
118. J. S. Theilacker (Consultant)
119. K. D. Timmerhaus (Consultant)
120. A. K. Williams (Consultant)
121. ORNL Y-12 Technical Library, Document Reference Section
122-123. Central Research Library
124. Laboratory Records
125. Laboratory Records, ORNL-RC
126. ORNL Patent Office
127. Nuclear Safety Information Center

External Distribution

128. Director, Reactor Division, DOE-ORO, P. O. Box E, Oak Ridge, TN 37830
129-130. Director, Division of Nuclear Fuel Cycle and Production, DOE, Washington, D.C. 20545
131-132. Director, Division of Reactor Research and Development, DOE, Washington, D. C. 20545
133. M. L. Bleiberg, Westinghouse Electric Corporation, Advanced Reactors Division, Waltz Mill Site, P. O. Box 158, Madison, PA 15663
134. Duane E. Clayton, Battelle Pacific Northwest Laboratory, P. O. Box 999, Richland, WA 99352
135. Martin Freidland, Gulf & Western Advanced Development and Engineering Center, 101 Chester Road, Swarthmore, PA 19081
136. Jerry M. Freidman, Sandia Laboratories, P. O. Box 5800, Albuquerque, NM 87115
137. Frank J. Jones, Bechtel Corporation, P. O. Box 3965, San Francisco, CA 94119
138. B. F.Judson, Vice-President and Manager, GEUMCO-Engineering, 175 Curtner Avenue, Mail Code 858, San Jose, CA 95125
139. R. S. Karinen, Programmed and Remote Systems Corporation, 3460 Lexington Avenue, St. Paul, MN 55112
140. Robert H. Karlsson, Rockwell International, Atomics International Division, Rocky Flats Plant, P. O. Box 464, Golden, CO 80401
141. R. E. Mullen, Aerojet Manufacturing Company, 601 South Placentia Avenue, P. O. Box 4210, Fullerton, CA 92634
142. L. A. Neimark, Argonne National Laboratory, 9700 South Cass Ave., Argonne, IL 60439
143. D. E. Wood, Kaman Sciences Corporation, 1500 Garden of the Gods Road, P. O. Box 7463, Colorado Springs, CO 80933
144. Research and Technical Support Division, DOE-ORO, P. O. Box E, Oak Ridge, TN 37830
145-353. Given distribution as shown in TID-4500 under UC-79c, Fuel Recycle Category (Applied).